25th ABCM International Congress of Mechanical Engineering
October 20-25, 2019, Uberlândia, MG, Brazil

COB-2019-1105
NUCLEATE BOILING FLOW AT LOW PRESSURE AND VELOCITY CONDITIONS BY THE RPI BOILING MODEL

Caio Pinheiro Carvalho
Post Graduating of PPGEE (Pós Gradução em Engenharia de Energia), Universidade Federal de São João Del Rei, Praça Frei Orlando, 170, São João del-Rei, Brazil
caiocpinheiro@hotmail.com
Luís Antônio Scola
Gustavo Rodrigues de Souza
Felipe dos Santos Loureiro
Department of Thermal and Fluid Sciences, Federal University of São João Del Rei, Praça Frei Orlando, 170, São João del-Rei, Brazil
scola@ufsj.edu.br
souzagr@ufsj.edu.br
felipe.loureiro@ufsj.edu.br

Abstract. *The advancement of computers and CFD (Computational Fluid Dynamics) allowed a rapid development in the computational modeling of nucleated boiling, phenomenon present, for instance, in engines cooling process, reactors and in the casting process. Among the developed models to describe the boiling, the RPI model (Rensselaer Polytechnic Institute) shows to be quite general and applicable in a great deal of cases; nevertheless, the interaction between phases (liquid and vapor) makes the model sensitive to some parameters such as velocity, pressure and turbulence. In this study, subcooled boiling heat transfer in an internal flow was numerically analyzed by the Ansys Fluent® software and the RPI wall boiling model was applied to low pressure and velocity conditions. Various combinations for wall functions using the k-ε turbulence model were studied with an operating condition of velocity and pressure ranging from 0.25 to 1 m/s and from 0 to 2 bar, respectively. The numerical simulations were validated by comparing with a literature experiment. The computational results show a good agreement with the experimental data and evidenced the influence of the selected wall function for this application.*

Keywords: *CFD, RPI Boiling Model, Nucleated Boiling, Turbulence, Wall Function.*

1. INTRODUCTION

Boiling in a subcooled liquid refers to the regime where a region of the flow is in contact with a surface temperature higher than the liquid saturation temperature, but the region of bulk flow is at a lower temperature. As a result, the formed bubbles detach from the surface and return to liquid phase when they reach a colder region. This phenomenon allows a higher heat transfer to be absorbed by the cooling fluid from a hot wall. However, a vapor film may be formed on the solid surface when the heat transfer exceeds the nucleated boiling limit, in such a condition, the heat of the fluid that flows to the cooling fluid drops abruptly and, as a result, high temperature zones start on the wall and can lead the system to collapse.

With the technology advancement and the improvement of computational capacity, this phenomenon starts to be exploited through numerical simulations and implemented in several engineering applications, such as nuclear reactor cooling and internal combustion engines. The possibility to determine the flow operating regime can ensure greater cooling efficiency and prevent further damage.

The first equations developed to model the nucleated boiling regime presented constant use of dimensionless parameters and empirical data. In addition, they are often applied only in restricted conditions in regimes close to what they were well-tried. This happens due to the high complexity of heat transfer mechanism between a hot surface and a bubble flow (multiphase). However, with the advancement of computational processors and the use of Computational Fluid Dynamics (CFD) tools, new models have appeared in the last three decades, advancing in solving general problems.

Among the most applied, some empirical models that depart from the classic model proposed by Rohsenow (1952), as in the researches of Dhir (1991), Fujita (1992) and variations of Chen (1966) model as the model proposed by Robinson and Hawley (2004) were applied. Finally, the RPI (Rensselaer Polytechnic Institute) model proposed by Kurul and Podowski (1991) considers that heat transfer between the hot surface and the flow is the sum of the convection, boiling

and quenching caused by the bubble departure dynamics. The RPI model has been implemented in models for analysis through finite volumes and applied commercially in the development of new products. However, some factors related to boiling behavior such as turbulence, geometry and parameters such as speed and pressure can affect the boiling process and should be considered in any type of application. Considering that the modeling of the boiling phenomenon is still in development and the fact that in many of these models there is a significant level of empiricism, it is necessary to understand the scope of each one of them, or in view of the circumstances of the parameters outside the boiling point, such models can yield good results.

Konkar et al. (2004) obtained local parameters for two-phase flow (void fraction and bubble size) under low pressure nucleated boiling conditions for flow through vertical channels. They could also evaluate the sensitivity of the other auxiliary models. Krepper et al. (2007) proved that the boiling model RPI is capable to calculating the mean cross-section steam volume fraction in heated vertical tubes with good agreement with published experimental data and to predicting the position where bubble departure can occur using a simple method. Punekar and Das (2013) adapted the model proposed by Chen (1966) for CFD application through the FLUENT software and simulated the experiment of Robinson and Hawley (2004) obtaining results with good accuracy.

Regarding to the influence of other parameters in nucleated boiling process analysis, some published studies show the sensitivity between the models. Koncar and Matkovic (2012) studied the development of the velocity field and the turbulence intensity in the hot wall region of a nucleated boiling vertical duct using HFE-301 as the cooling fluid. The turbulent model used was Shear Stress Turbulent (SST). The results showed good agreement with respect to heat transfer and Reynolds number variation and experimental data, but the velocity and turbulence magnitude did not. The authors also studied the influence of surface roughness with velocity and turbulence in the wall region. The inclusion of a simple turbulence model improved the correlation of the results. Zhang et al. (2015) compared the turbulence models k-ε and k-ω and their many variations when applied in the forced convection flow modeling and subcooled boiling in a vertical tube using the RPI model. In addition, they analyzed the performance of the dispersed treatments and per phase of the turbulence in the multiphase flow.

The studies of Koncar and Matkovic (2012) and Zhang et al. (2015) have shown the importance of an adequate modeling of the turbulence for a nucleated boiling model, especially with regard to analysis close to the heated region. Most of the work focused on vertical duct flow, common features in industrial cooling process and nuclear reactors. However, another application where the nucleated boiling regime can be used as an improvement for thermal exchange is in internal combustion engines. In this case, the flow crosses galleries of complex geometries in several directions, and presents a low velocity (flow of maximum 10 m/s) and low pressure (typically 1 bar) (Heywood, 1988). In this sense, Punekar and Das (2013) obtained good results for the simulation in typical conditions of motor cooling system using the model proposed by Chen (1966) by reproducing the Robinson and Hawley (2004) experiment. However, the analysis of the turbulence models, wall functions, mesh and other points that may influence the result were not evaluated.

In this work, a comparison between the wall functions (Enhanced, Standard and Non-equilibrium) using Realizable k-ε Turbulence Model applied to a forced convection flow under a nucleated boiling regime of subcooled liquid, in a horizontal duct, was carried out. As a comparative and evaluative parameter, the data obtained by the experimental model of Robinson and Hawley (2004) were adopted as a reference. They evaluated experimentally and through computational simulation a variation on the classical Chen's model, proposing the inclusion of parameters such as roughness. Such evaluation is considered for velocities between 0.25 and 1 m/s and pressures from 0 to 2 bar, an operating condition typically presented in cooling flows in internal combustion engines. The computational modeling was performed using the Ansys Fluent® software v18.1. Student Version, a well-known software for the analysis of fluid dynamics and heat transfer systems using the finite volume method that contains a vast library of physical and computational models.

2. MODELS FOR SUBCOOLED BOILING FLOW

The water-vapor two-phase flow in the tube was simulated in the Eulerian-Eulerian framework. The mass, momentum and energy equations were established for each phase separately (Tong and Tang, 1997). Interactions between the phases are taken into account using inter-phase force models and heat transfer models. At the vicinity of the wall, the inlet subcooled liquid phase is heated by the hot wall and vapor bubbles are generated on the wall surface. The heat and mass transfers near the wall surface need to be accurately modeled. The RPI wall boiling model proposed by Kurul and Podowski (1991) is used to describe the near-wall heat transfer of the subcooled boiling flow. Besides, Standard, Non-Equilibrium and Enhanced Wall Functions were compared using the Realizable k-ε model. The governing equations and auxiliary equations are given in the following of this section.

2.1 Governing Equations

Governing equations of Eulerian two-phase model include mass, momentum and energy equations for each phase, i.e.,

Mass equation:

$$\nabla.(\alpha_r \rho_r \boldsymbol{u}_r) = \dot{m}_{sr} - \dot{m}_{rs} + S_r \tag{1}$$

where α_r, ρ_r, $\boldsymbol{u}_r$ and S_r are, respectively, the void fraction, the density, the velocity vector and the source term of the phase *r*. Moreover, $\dot{m}_{rs}$ and $\dot{m}_{sr}$ are the rate of condensed and evaporated mass between the phases.

Momentum Equation:

$$\nabla.(\alpha_r\rho_r\boldsymbol{u}_r \otimes \boldsymbol{u}_r) = \alpha_r\rho_r\boldsymbol{g} - \alpha_r\nabla p + \nabla.\boldsymbol{\tau}_r + \dot{m}_{sr}\boldsymbol{u}_{sr} - \dot{m}_{rs}\boldsymbol{u}_{rs} + \boldsymbol{F}_{sr} + \boldsymbol{F}_{slift} \quad (2)$$

where $\boldsymbol{g}$ represents the gravity vector, $\boldsymbol{\tau}_r$ represents the stress tensor for the phase *r*. In addition, $\boldsymbol{u}_{sr}$ and $\boldsymbol{u}_{rs}$ are the velocity vectors on the interface, while $\boldsymbol{F}_{sr}$ and $\boldsymbol{F}_{sr}$ are, respectively, the force vector on the interface and the lift force vector as discussed later on.

Energy Equation:

$$\nabla.(\alpha_r\rho_r\boldsymbol{u}_rH_r) = \nabla.(\alpha_rk_r\nabla T_r) + \dot{m}_{sr}H_{sr} - \dot{m}_{rs}H_{rs} + Q_{sr} \quad (3)$$

where H_r and k_r represent, respectively, the specific enthalpy and the thermal conductivity of the phase *r*. On the interface, H_{rs} and H_{sr} are the enthalpy changes when vapor is condensing and the liquid is evaporating. The term Q_{sr} represents the interfacial heat transfer between the phases, which, for subcooled boiling where the vapor temperature is assumed constant, is due to only the liquid phase and, thus, $Q_{rs} = 0$.

2.2 RPI Boiling Model

In the RPI wall boiling model, the heat transfer in the flow from the wall to the liquid is divided into three components; namely, the convection heat flux, the quenching heat flux and the heat flow of evaporation, i.e.:

$$q_w = q_C + q_Q + q_E \quad (4)$$

The heated surface is subdivided into two ratios of areas. A ratio A_b and another (1-A_b), which are the regions covered by bubble and liquid, respectively. In this way, the convective heat flux, q_C, is expressed by:

$$q_C = h_r(T_w - T_r)(1 - A_b) \quad (5)$$

where h_r is the convective coefficient of the fluid, and T_w and T_r are the wall and liquid temperatures, respectively. In addition, $A_b = KN_w\pi D_w^2/4$ in which $K = 4.8\exp(-Ja_{sub}/80)$ is an empirical constant, $Ja_{sub} = \rho_r c_{pr}(T_{sat} - T_r)/(\rho_s h_{rs})$ is the subcooled Jacob number, where T_{sat} is the saturation temperature.

The N_w is the density of the nucleation site, represented by a correlation based on surface overheating $N_w = C^n(T_w - T_{sat})^n$ where C = 210 and n = 1,805 (empirical parameters proposed by Lemmert and Chawla (1977)). D_w is the bubble detachment diameter based on empirical correlations given by $D_w = \min(0.0014, 0.0006e^{-\frac{\Delta Texc}{45.0}})$.

The heat transfer in the flow by cooling, q_Q, models the average of the transient cycle of heat transfer relative to the moment when the liquid occupies the region of the wall when the bubble is released, and its expression is given by:

$$q_Q = \frac{2k_r}{\sqrt{\pi\lambda_r P}}(T_w - T_r) \quad (6)$$

where k_r represents the conductivity of the liquid phase, P is the periodic time, and $\lambda_r = k_r/\rho_r C_{pr}$ is the thermal diffusivity.

The heat transfer due to the evaporative flow, q_E, is given by:

$$q_E = V_d D_w \rho_s h_{rs} f \quad (7)$$

where V_d is the volume of bubbles based on the peel diameter and f is the bubble detachment frequency.

From these basic equations of the model, one must define each of the parameters used. The following relationship is also implemented and based on the Del Valle and Kenning (1985) model. The frequency of bubble departure is given by the equation below based on the inertia of a controlled growth. This model was presented by Cole (1960).

$$f = \frac{1}{P} = \sqrt{\frac{4g(\rho_r - \rho_s)}{3\rho_r D_w}} \tag{8}$$

2.2 Interfacial Heat Transfer

For flows between two fluids, be it a gas and a liquid or between two liquids, a phase must be chosen as primary, that is, the one that represents the largest volume within the total control volume (i.e., the liquid phase represented by *r* hereafter). The second phase is assumed to form droplets or bubbles. The exchange coefficient for these types of mixtures, present in momentum equation (2) can be written as follows:

Drag Interaction:

$$\boldsymbol{F}_{rs} = \frac{C_D A_b \mu_r Re}{8 d_s}(\boldsymbol{u}_s - \boldsymbol{u}_r) \tag{9}$$

where C_D represents the drag coefficient, d_s is the average bubble diameter and μ_r is the liquid phase viscosity, Re is the relative Reynolds number based on the average bubble diameter.

The model proposed by Ishii (1979) is used for the drag coefficient. In this model, the drag coefficient C_D is determined by the lowest value between drag of the viscous regime C_D^{vis} and the distorted regime C_D^{dis}, defined as follows:

$$\begin{aligned} C_D &= \min(C_D^{vis}, C_D^{dis}) \\ C_D^{vis} &= \frac{24}{Re}(1 + 0.15Re^{0.15}) \\ C_D^{dis} &= \frac{2}{3}\frac{d_s}{\sqrt{\frac{\sigma}{g(\rho_s - \rho_r)}}} \end{aligned} \tag{10}$$

where Re is the relative Reynolds number, σ is the surface stress between the phases (ANSYS Fluent Solver Theory Guide, 2006).

The model that characterizes the bubble lift in the flow was proposed by Moraga et al. (1999). In this model, the lift coefficient combines the opposing actions of two phenomena; namely, the classical lift resulting from the interaction between the vapor bubbles and the liquid phase and that from the increase induced by the vorticity caused by the interaction between the bubbles and the vortices released by it. As a result, the lift coefficient is defined in terms of the Reynolds number of the bubbles as well as the Reynolds number of the vortices caused by it.

Lift Interaction:

$$\boldsymbol{F}_{slift} = -C_l \rho_s \alpha_r (\boldsymbol{u}_s - \boldsymbol{u}_r) \times (\nabla \times \boldsymbol{u}_s) \tag{11}$$

$$Re_r = \frac{\rho_r |\boldsymbol{u}_s - \boldsymbol{u}_r| d_r}{\mu_s} \tag{12}$$

$$Re_w = \frac{\rho_r |\nabla \times \boldsymbol{u}_s| d_r^2}{\mu_s} \tag{13}$$

Defining $\varphi = Re_r Re_w$, Moraga's coefficient is defined by:

$$C_l = \begin{cases} 0.0767 & \varphi \leq 6000 \\ -\left(0.12 - 0.2e^{-\frac{\varphi}{3.6}\times 10^{-5}}\right) e^{\frac{\varphi}{3}\times 10^{-7}} & 6000 < \varphi < 5 \times 10^7 \\ -0.6353 & \varphi \geq 5 \times 10^7 \end{cases} \tag{14}$$

2.3 Interfacial Mass and Heat Transfer

When the bubble starts from the hot surface and moves to condensation, the heat exchange is represented by the following equation:

$$q_l = q_{cond} = h_{ri} A_i (T_{sat} - T_r) \tag{15}$$

where A_i represents the proportion of the interface area defined as $A_i = 6\alpha_s / d_b$, with d_b being the local bubble diameter and h_{ri} is the convective coefficient of the heat exchange at the interface given by:

$$h_r = k_r Nu_r / d_b \tag{16}$$

where Nu_r is the Nusselt number of the liquid phase calculated by the equation of Ranz and Marshall (1952) as follows:

$$Nu_r = 2 + 0.6 Re_s^{0.5} Pr_r^{1/3} \tag{17}$$

where Re_s is the Bubble Reynolds number and Pr_r is the Prandtl number of the liquid phase.

The mass flow interaction terms, presented in Equations (1), (2) and (3), represent the vaporization and condensation. The primary source of the steam bubbles is generated by the hot wall. The mass of steam generated from the hot wall is given by:

$$\dot{m}_{rs} = \dot{m}_{vap} = \frac{\pi D_w^3}{6} \rho_s f N_w \tag{18}$$

In the RPI model, it is assumed that the vapor maintains the saturation temperature and the mass transfer rate can be expressed by:

$$\dot{m}_{sr} = \dot{m}_{cond} = \max\left(\frac{q_{cond}}{h_{rs}}, 0\right) \tag{19}$$

The diameter of the local bubble, d_b, is a function of local boiling. The following correlation is used to compute d_b.

$$d_b = \begin{cases} max\left[1.0 \times 10^{-5}, d_{min}\, exp\left(\frac{-K(\Delta T_{sub} - \Delta T_{max})}{d_{min}}\right)\right] & \Delta T_{sub} > 13.5K \\ d_{max} - K(\Delta T_{sub} - \Delta T_{min}) & \Delta T_{sub} \leq 13.5K \end{cases} \tag{20}$$

where $d_{min} = 0.000015m$, $d_{max} = 0.001$, $\Delta T_{min} = 0$ K, $\Delta T_{max} = 13.5$ K and $K = \frac{d_{max} - d_{min}}{\Delta T_{max} - \Delta T_{min}}$

3. METHODOLOGY

In order to analyze the main features of the model, the data applications and the direct and indirect parameters of the problem, as the computational bases were divided in two steps. The first step, the experiment proposed by Robinson and Hawley (2004) is reproduced computationally using the RPI model for a nucleated boiling. The experiment considers flows through a rectangular section duct where a heated plate is mounted at the bottom of the duct, raising the temperature to the boiling point of the flow. The details of the experiment are presented in the following sections. The results are compared with those of the empirical model by the same author and his experiments. In this step, the analysis of the model for an application in low pressure flows is carried out. In the second step, adopting the same computational model, wall functions are evaluated and compared. Parameters such as plate temperature and bubble formation rate are also evaluated.

Based on the model proposed by Chen (1966), Robinson and Hawley (2004) developed an empirical model of nucleated boiling in order to better estimate the heat transfer in flows inside the cooling galleries of internal combustion engines. The details of the developed equations were presented in section 2.2. In order to validate the developed model, a device was created to obtain the experimental data according to Figure 3. This device was created with the pretension of better reproduce the flow regime that happens inside the gallery of a combustion engine.

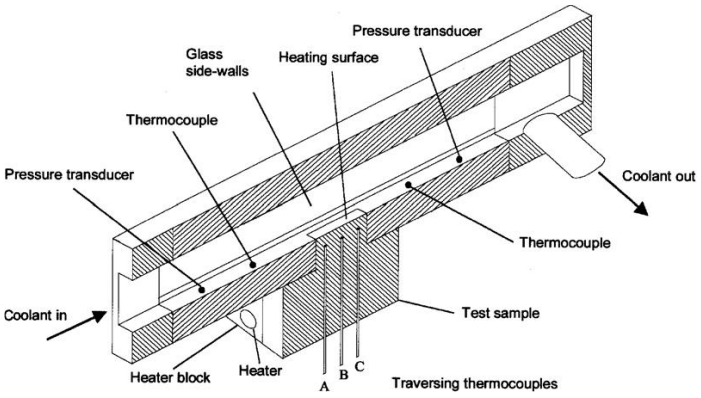

Figure 1 – Robinson and Hawley (2004) experimental apparatus.

As shown in Figure 1, a rectangular duct of 16x10 mm² section and 241 mm length was employed. A heated surface (region of heat flow) of 10x50 mm² is positioned at the bottom of the channel and located at 76 mm from the entrance. Thermocouple sensors were installed 2 mm from the heated surface and also at the inlet and outlet of the duct. In addition, pressure transducers monitor the input and output of the system. The flow enters and exits the duct as shown in Figure 1. For this experiment, a mixture of water and ethylene glycol in the ratio of 1 to 1 was used as the cooling fluid. This compound is commonly used in the automotive industry in the engine cooling system. Table 1 shows the thermophysical properties of the cooling fluid.

Table 1. thermophysical properties adopted for Water/ Ethylene Glicol 1 to 1 ratio.

Thermophysical properties	
Density	$\rho = 1079.1 - 0.6169\mathrm{T}\ kg/m\hat{}3$
Thermal Conductivity	$k = 0.3746 + 0.0006\mathrm{T}\ W/mK$
Viscosity	$\mu = 0.0065e\hat{}(-0.0241\mathrm{T})\ kg/ms$
Specific Heat	$C_P = 3220.2 + 4.4286\mathrm{T}\ J/kgK$

The results obtained in the experiments of Robinson were used to validate his mathematical model and both are used here for the correlation of this present work.

In this work, wall functions, including Standard, Menter, Enhanced and Non-Equilibrium, are investigated since they are the most widely used models in engineering applications. Different models need different near-wall mesh resolution, or the so-called y^+. As well-known, the near-wall region can be subdivided into three sublayers, i.e., viscous sublayer, buffer layer and fully turbulent region. For *k-ε* models with wall functions, near-wall grid must locate in the fully turbulent region, which means the viscosity-affected region (viscous sublayer and buffer layer) is not resolved. Thus the $y^+$of near-wall mesh must be larger than 11.225 in this situation. When the grids are such that y^+<11.225 at the wall-adjacent cells, the solution accuracy cannot be maintained (Launder and Spalding (1972); Orszag et al. (1993); Shih et al. (1995)). However, as noted in FLUENT theory guide, Ansys (2012), *k-ε* model can deal with meshes with near-wall y^+ less than 11.225 with the help of enhanced wall function.

Anyway, four sets of grids are employed in this work to check the convergence and correlation for a multiphase analysis. Table 2 shows the details of each grid, including the cell number, the mean cells size and the resultant dimensionless near wall y^+. As can be seen, M1 and M2 satisfy the constraint that y^+ be larger than 11.225, whereas in M4 such a value is near to 1. However, some of the wall-adjacent meshes of ICM3 are located in the buffer layer.

Table 2. Grid Details.

Grid	Nodes	Elements	Mean Cell Size	Calculated Near-Wall Y^+
M1	20.358	16608	1.4 mm	8 - 17 (0.25 m/s) 21 – 30 (0.5 m/s) 39 – 52 (1.0 m/s)
M2	47.916	40970	1.0 mm	9 – 14 (0.25 m/s) 17 – 24 (0.5 m/s) 37 – 47 (1.0 m/s)
M3	74.052	66998	1.0 mm (2 near-wall elements)	3 – 4 (0.25 m/s) 6 – 8 (0.5 m/s) 9 – 10 (1.0 m/s)
M4	113.256	106040	1.0 mm (5 near-wall elements)	< 1

4. COMPUTATIONAL DOMAIN, BOUNDARY CONDITIONS AND NUMERICAL METHOD

In the comparative analysis with the Robinson and Hawley experimental model, some of the conditions used in the authors' experiments were adopted. To simulate the tests performed, the boundary conditions were adopted like the model presented in Figure 2. Table 2 presents the conditions of the analyzes. Table 3 presents a summary of the analyzed cases where STA, NON, MEN and ENH represent the Standard, Non-Equilibrium, Menter and Enhanced wall functions respectively, and the pressure in bar represents the pressure adopted.

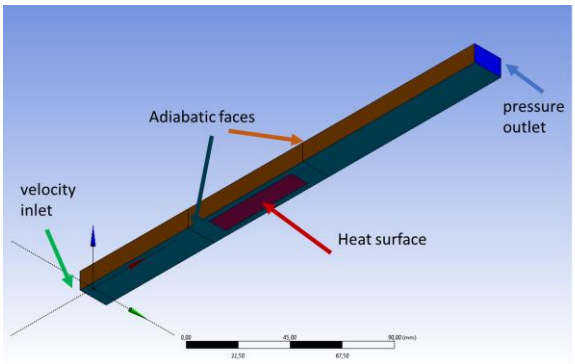

Figure 2 – Boundary Conditions.

Table 3. Boundary Conditions Values.

Inlet Temperature	Inlet Velocity	Pressure Outlet (Relative)	Heat Flux	Boiling Temperature
90°C	*0.25 / 0.5 / 1* m/s	0 / 1 / 2 (bar)	*0 – 1500* kW/m²	*127* °C

Table 4. Resume of Cases Analyzed.

Velocity	M1	M2	M3	M4
0.25 m/s	*Standard* – 1 bar	*Standard* – 0 bar *Standard* – 1 bar *Standard* – 2 bar *Non- Equilibrium* – 1 bar *Menter* – 1 bar *Enhanced* – 1 bar	*Standard* – 1 bar	*Standard* – 1 bar
0.5 m/s	*Standard* – 1 bar	*Standard* – 1 bar	*Standard* – 1 bar	*Standard* – 1 bar
1.0 m/s	*Standard* – 1 bar	*Standard* – 1 bar	*Standard* – 1 bar	*Standard* – 1 bar

Regards numerical aspects, the Phase Coupled SIMPLE (PC-SIMPLE) is an extension of the SIMPLE algorithm to multiphase flows. The velocities are solved coupled by phases in a segregated fashion. Fluxes are reconstructed at the faces of the control volume and then a pressure correction equation is built based on total continuity. The coefficients of the pressure correction equations come from the coupled per phase momentum equations. The gradient terms are discretized by least squares cell based method. All other terms in governing equations are discretized by second-order upwind method.

5. RESULTS AND DISCUSSION

5.1 Mesh Convergence Analysis

As previously mentioned, there is a range of y^+ value suggested for each wall function. For *k-ε* turbulence model, the wall functions work well between 10 and 100 generally, although the y^+ is calculated by the ratio between mesh length plus friction velocity and kinematic viscosity, so that, the changing of flow velocity will impact on its value. To understand the real impact of mesh, the values were varied conform Table 2.

Figure 3 shows a convergence between the results from the mesh with edges of 1 mm and without refinement in the wall. Another important point is that models with refinement close to the wall do not converge from certain values for the heat flow. This worsens for lower speeds and for greater refinement in the wall. The values of y^+ calculated for all cases

using the 1 mm mesh are in the range recommended for application of the wall functions that will be analyzed, validating their use.

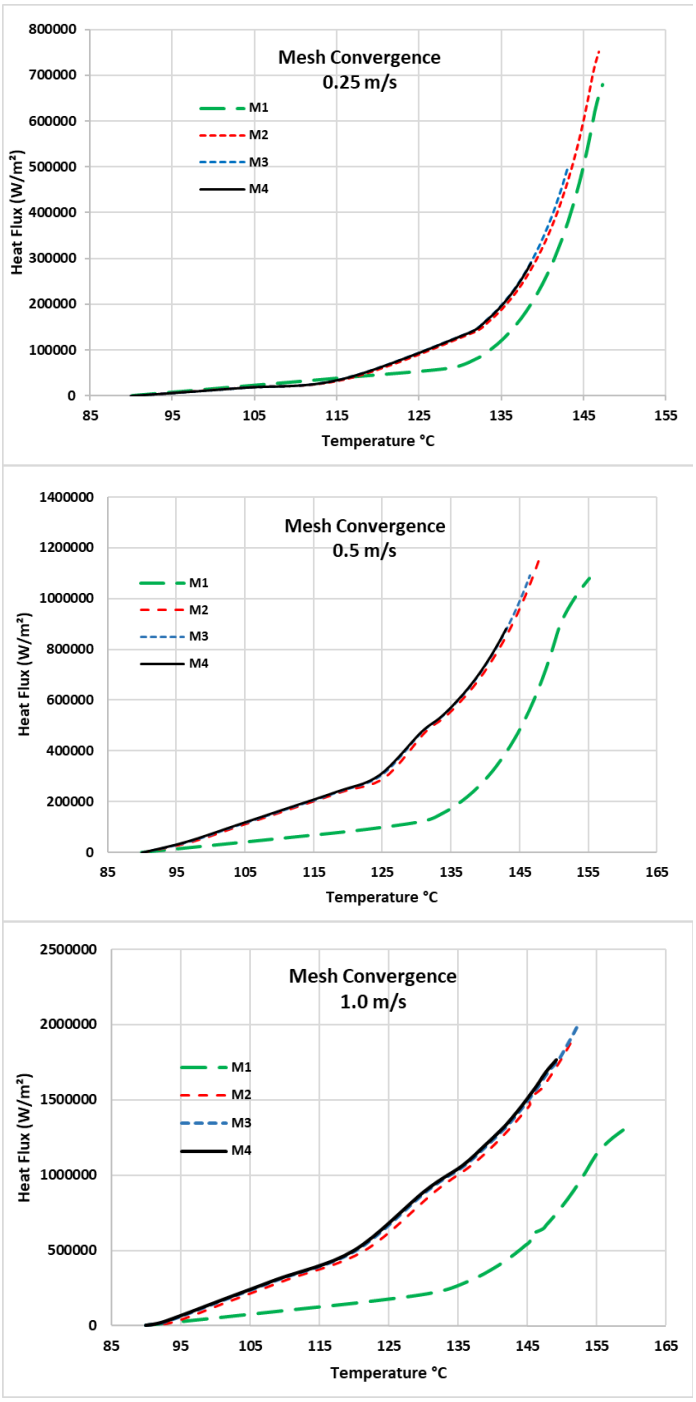

Figure 31- Mesh Convergence

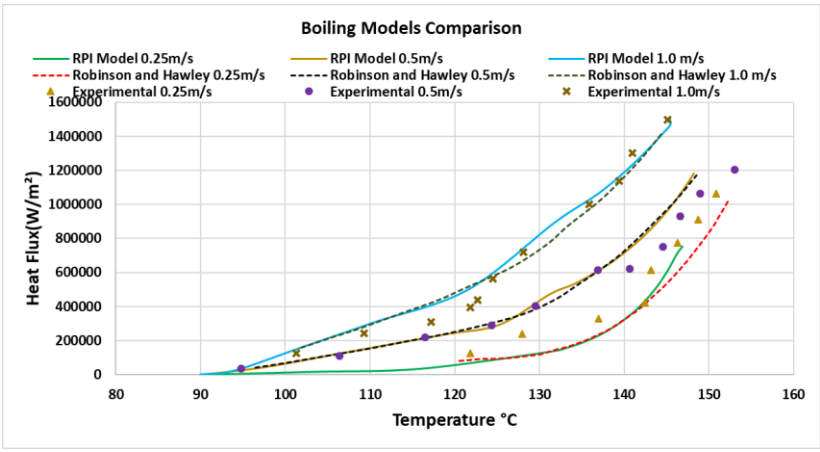

Figura 4 Boiling Models Comparison

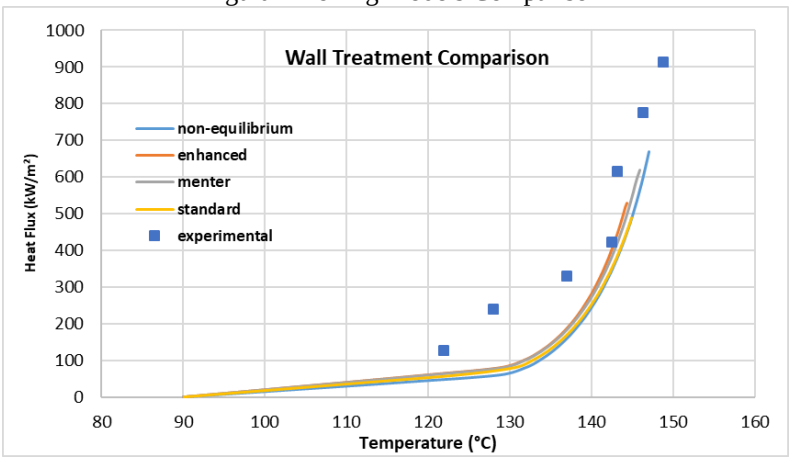

Figura 5a - Wall Function Comparison

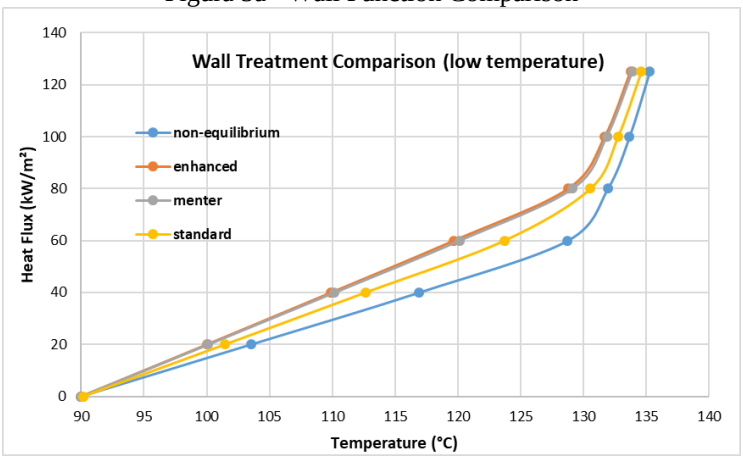

Figura 5b - Wall Function Comparison (Low Temperatures)

5.2 Accuracy and Effects of Velocity

After the mesh convergence, the results are compared with those obtained in the study of Robinson and Hawley (2004). The parameters were maintained in relation to the previous analyzes. Figure 4 shows the curves obtained for the velocities of 0.25 m/s, 0.5 m/s and 1 m/s for the RPI model, an empirical model proposed by Robinson and Hawley based on the classic model of Chen (1966) and the experimental model of the same authors.

When compared to the experimental model, the results obtained through the RPI model show a good correlation in all cases. A greater deviation is observed for temperatures between 110 °C and 120 °C and speed of 1 m / s. The same is true

for speeds greater than 140 °C at 0.5 m/s and for lower temperatures at 0.25 m / s. However, comparing the empirical model proposed by Robinson and Hawley and the RPI model, the results are similar for all cases.

5.3 Temperature and Vapor Distribution

Nucleate boiling starts at a temperature of 127 °C and 1 bar of pressure for water and ethylene glycol. In Figure 4 the curve transition is easy to be noted for 0.25 m/s in this temperature, however, for higher velocities, the effects of convection make the transition not so perceptive once the boiling heat transfer decrease with the increase of convection. The flow velocity tends to reduce the bubble formation.

Figure 6 shows the volume fraction and temperature field for 600 kW/m² heat flux for 0.25 m/s, 0.5 m/s and 1 m/s in the heated surface and near regions (in such a figure the flow is from right to left).

5.3 Wall Function Comparison

The analyzed velocity was 0.25 m/s, where the effects of boiling are more pronounced. We chose the Realizable model for turbulence. The analyzed wall functions were Enhanced, Non-Equilibrium, Menter and Standard. Figures 5a and 5b show the results obtained, whereas Figure 5b shows the detail results for lower temperatures.

The wall functions showed similar behavior mainly at temperatures above the boiling point. The figure shows that the standard and enhanced models diverged for heat fluxes greater than 500 kW / m², whereas the non-equilibrium model converged to flows close to 700 kW / m². Figure 5b shows in detail the difference of the results for temperatures between 100 and 130 °C, in this region the non-equilibrium model reaches temperatures of 4 to 9 °C higher than the enhanced and menter models. This implies different heat flows to achieve boiling in each case. However, with the increase of the heat transfer by boiling, the models will present similar behavior with a maximum difference of 4 °C to 80 kW/m² and that tends to reduce in greater heat flows. The results demonstrated that the RPI model is slightly influenced by the wall functions and the turbulence model, however, in temperature bands where the heat exchange is mainly carried out by forced convection, the wall function has a determining effect on the result.

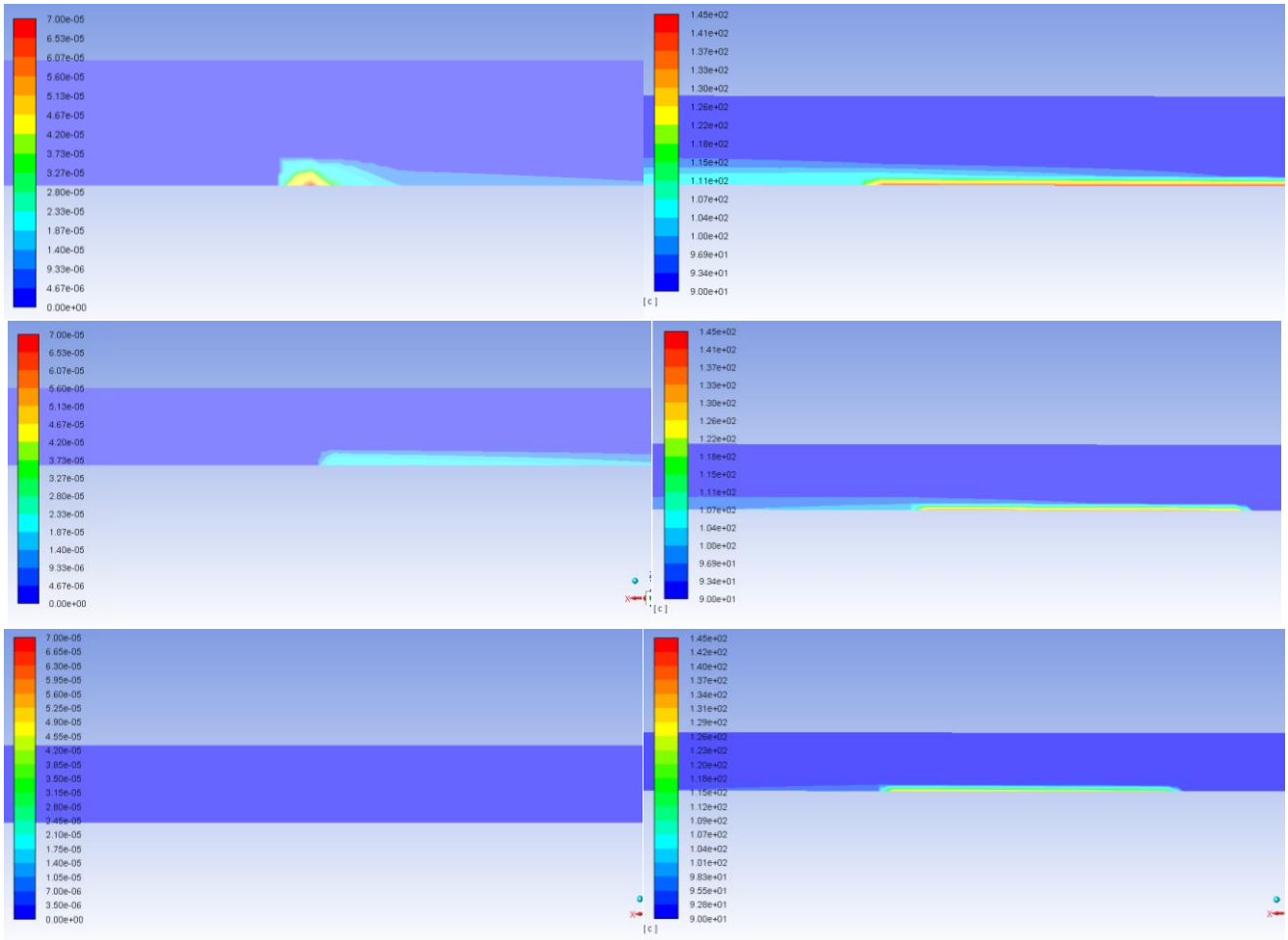

Figura 6 - Volume Fraction (left) and Temperature field (right) for 600 kW/m² (0.25 m/s, 0.5 m/s, 1.0 m/s)

6. CONCLUSIONS

Bearing in mind the obtained results, conclusions can be drawn regarding the behavior of the RPI model for analyses at low pressure and velocity conditions as well as on the modeling of multiphase flow in general.

The graphs comparing the velocity variation, between 0.25, 0.5 and 1.0 m/s, present results equivalent to those obtained by the model proposed by Robinson and Hawley and satisfactory when compared to the experimental one. Despite some scattered points obtained in the experimental analysis, it is clear that the simulation reached the objective of predicting the trend of the nucleated boiling phenomenon.

Regarding the wall functions for the turbulence model, the results demonstrated that the RPI model is little influenced by the wall functions and the turbulence model; however, in temperature bands where the heat exchange is mainly carried out by forced convection, the wall function has a determining effect on the result and point of vaporization.

7. REFERENCES

Chen, C., "Correlation for boiling heat transfer to saturated fluids in convective flow". I&EC – Process Des. Dev., 5(3), 322, 1966.

Cole, R., A Photographic Study of Pool Boiling in the Region of the Critical Heat Flux. AIChE J. 6. 533–542, 1960.

Del Valle, V. H., Kenning, D. B. R., "Subcooled flow boiling at high heat flux, International Journal of Heat and Mass Transfer", vol. 28, no. 10, pp. 1907–1920, 1985.

Dhir V. K., Nucleate and transition boiling heat transfer under pool and external flow conditions. Int. J. Heat Fluid Flow 12(4): 290–314, 1991.

Fujita, Y., The state of the art—nucleate boiling mechanism. See Dhir & Bergles, pp. 83–98, 1992.

Ishii, M., Two-fluid model for two-phase flow. 2nd International Workshop on Two-phase Flow Fundamentals. RPI, Troy, NY, 1979.

Koncar, B., Matkovic, M., "Simulation of turbulent boiling flow in a vertical rectangular channel with one heated wall". Nuclear Engineering and Design 245 131-139, 2012.

Krepper, E., Koncar, B., Egorov, Y., CFD modelling of subcooled boiling—concept, validation and application to fuel assembly design. Nucl. Eng. Des. 237,716–731, 2007.

Kurul, N., Podowski, Z., "On the modeling of multidimensional effects in Boiling channels". 27th National Heat Transfer Conference, Minneapolis, Minnesota, USA, 1991

Lemmert, M., Chawla, M., Influence of flow velocity on surface boiling heat transfer coefficient in Heat Transfer in Boiling. E. Hahne and U. Grigull, Eds., Academic Press and Hemisphere, New York, NY, USA, 1977.

Moraga, J., Bonetto, T., Lahey, T., Lateral forces on spheres in turbulent uniform shear flow. International Journal of Multiphase Flow. 25. 1321–1372, 1999.

Robinson, K., Hawley, J.G., N.A.F., "Experimental and Modeling Aspects of Flow Boiling Heat Transfer for Application to Internal Combustion Engines". Proc. Instn Mech. Engrs Vol. 217 Part D: Automobile Engineering, 2004.

Rohsenow, M., A Method of Correlating Heat Transfer Data for Surface Boiling of Liquid. Trans. ASME, 74, 969, 1952.

Tong, L.S and Tang, Y.S., "Boiling Heat Transfer and Two-Phase Flow". Series in Chemical and Mechacanical Engineering, 1997.

Zhang, R., Cong, T., Tian, W., Qiu, S., Su, G., "Effects of turbulence models on forced convection subcooled boiling in vertical pipe". Annals of Nuclear Energy 80 293-302, 2015.

8. RESPONSIBILITY NOTICE

The authors are the only responsible for the printed material included in this paper.